Denitrifying bioreactor clogging potential during wastewater treatment

Laura E. Christianson [a,*], Christine Lepine [b], Kata L. Sharrer [b], Steven T. Summerfelt [b]

[a] Department of Crop Sciences, University of Illinois at Urbana-Champaign, AW-101 Turner Hall, 1102 South Goodwin Avenue, Urbana, IL 61801, USA
[b] The Conservation Fund Freshwater Institute, 1098 Turner Road, Shepherdstown, WV 25443, USA

ABSTRACT

Chemoheterotrophic denitrification technologies using woodchips as a solid carbon source (i.e., woodchip bioreactors) have been widely trialed for treatment of diffuse-source agricultural nitrogen pollution. There is growing interest in the use of this simple, relatively low-cost biological wastewater treatment option in waters with relatively higher total suspended solids (TSS) and chemical oxygen demand (COD) such as aquaculture wastewater. This work: (1) evaluated hydraulic retention time (HRT) impacts on COD/TSS removal, and (2) assessed the potential for woodchip clogging under this wastewater chemistry. Four pilot-scale woodchip denitrification bioreactors operated for 267 d showed excellent TSS removal (>90%) which occurred primarily near the inlet, and that COD removal was maximized at lower HRTs (e.g., 56% removal efficiency and 25 g of COD removed per m^3 of bioreactor per d at a 24 h HRT). However, influent wastewater took progressively longer to move into the woodchips likely due to a combination of (1) woodchip settling, (2) clogging due to removed wastewater solids and/or accumulated bacterial growth, and (3) the pulsed flow system pushing the chips away from the inlet. The bioreactor that received the highest loading rate experienced the most altered hydraulics. Statistically significant increases in woodchip P content over time in woodchip bags placed near the bioreactor outlets (0.03 vs 0.10%P_2O_5) and along the bioreactor floor (0.04 vs. 0.12%P_2O_5) confirmed wastewater solids were being removed and may pose a concern for subsequent nutrient mineralization and release. Nevertheless, the excellent nitrate-nitrogen and TSS removal along with notable COD removal indicated woodchip bioreactors are a viable water treatment technology for these types of wastewaters given they are used downstream of a filtration device.

1. Introduction

Chemoheterotrophic denitrification is the most widely used nitrogen (N) removal process in wastewater treatment (Lu et al., 2014). Addition of a soluble carbon (C) source (e.g., methanol, acetate, ethanol, glycerol) fuels this anoxic step-wise microbial reduction of nitrate (NO_3^-) to dinitrogen (Tchobanoglous et al., 2003). Recent increasing concern about nutrient pollution from non-point sources and other non-regulated N streams has resulted in the expansion of denitrification technologies to include simple reactors filled with inexpensive and readily available solid organic C sources such as woodchips (Schipper et al., 2010). In agricultural settings, these woodchip denitrification bioreactors offer a targeted approach for passive N treatment from subsurface drainage, runoff, and greenhouse effluents (generally > 25% N removal, 2–20 g N removed per m^3 bioreactor per d; Christianson et al., 2012; Warneke et al., 2011; Woli et al., 2010).

Woodchip bioreactors are being examined in applications such as aquaculture facilities that have more controlled flow rates than non-point source N streams that have been the major application of bioreactors to date (Lepine et al., 2016; von Ahnen et al., 2016). Flushing of chemical oxygen demand (COD) and nutrients upon woodchip bioreactor start-up is a well-established phenomenon (Healy et al., 2012), but the opportunity to design these systems for more controlled flow rates (e.g., wastewater versus tile drainage water) raises the new question of how to minimize flushing impacts through design (i.e., through hydraulic retention time (HRT)). Moreover, because woodchip bioreactors have most widely been

used in the treatment of relatively low total suspended solids (TSS) and COD agricultural N sources (e.g., agricultural tile drainage), it is now vital to evaluate the impact of design flow rates on TSS and COD removal in woodchip bioreactor treatment of wastewater. Efficient filtration of wastewater TSS would be widely expected due to the rough surface area of the woodchips (Choudhury et al., 2016). However, conventional knowledge indicates that frequent woodchip replacement due to either C media exhaustion or media clogging potentially changes the economics of this low-cost denitrification option. Increasing interest from the aquaculture industry, in particular, necessitates better understanding of the potential for woodchip clogging as well as design HRT guidance for TSS and COD removal in woodchip denitrification bioreactors. The objectives of this work were to: (1) evaluate the HRT impacts on COD and TSS production or removal under start-up or longer-term operation, respectively, and (2) assess the potential for woodchip clogging to occur under this wastewater chemistry. Previous findings from this study include the first ever evaluation of woodchip bioreactor HRT for NO_3^- removal from aquaculture wastewater (Lepine et al., 2016) and assessment of phosphorus dynamics in the woodchips and wastewater (Sharrer et al., 2016).

2. Methods and materials

2.1. Bioreactor design and operation

Four pilot-scale woodchip denitrification bioreactors (Fig. 1; L × W × D:3.8 × 0.76 × 0.76 m; ≈1:10 scale based on surface foot print) were constructed of plywood, lined with plastic, and operated for 267 d at The Conservation Fund's Freshwater Institute research campus (Shepherdstown, WV, USA; May 2014 to February 2015; previously described by Lepine et al., 2016 and Sharrer et al., 2016). The woodchips were classified as a "3 inch, hardwood blend" by the local supplier (Lowe Products, Shepherdstown, WV), and had a D_{50} (median diameter) of 1.2 cm, porosity of 70%, and bulk density of 217 ± 11 kg/m^3 (mean ± SD).

The bioreactors were operated under a start-up phase which consisted of wastewater application on hourly pumping cycles (Phase I: d 1–162) and a phase with double the hydraulic loading rate (HLR) as Phase I with bioreactors dosed with the same volume of wastewater as during Phase I except twice per hour (Phase II: d 169–267). The four bioreactors were each operated under a different HRT and HLR, and the retention times during Phase II were approximately half that of Phase I (Phase I: 12, 24, 42, and 55 h HRT; Phase II: 6.6, 12, 20, and 29 h HRT). Hydraulic retention time (τ) for woodchip bioreactors is described as:

$$\tau = \frac{V_r * \rho}{Q} = \frac{Pore\ Volume}{Q} \qquad (1)$$

where Q is the reactor flow rate, V_r is the saturated volume of the reactor (3.8 × 0.76 × 0.61 m; Fig. 1), and ρ was woodchip porosity (70%) (Tchobanoglous et al., 2003). Lepine et al. (2016) previously reported N removal rates for these pilot-scale denitrification bioreactors were a function of HRT (g N removed per m^3 bioreactor per d = $17.3 + (111.2 * e^{(-0.22 * HRT)})$).

Wastewater (i.e., overflow from gravity thickening settlers used to dewater and capture waste biosolids) generated via the production of rainbow trout (*Oncorhynchus mykiss*) and Atlantic salmon (*Salmo salar*) in on-site recirculating aquaculture systems was pumped to a mixing tank where it was dosed with sodium nitrate to achieve bioreactor inflow of 25–80 mg NO_3^--N/L. The context for this study was treatment of aquaculture wastewater, thus it was most realistic to use effluent from the on-site fish culture system (e.g., wastewater microbiology, temperature, etc.,

consistent with a production fish culture system), but N dosing was required to produce realistic NO_3^- levels due to the efficiency of upstream N-removal unit processes at this research facility. The mixing tank solution was circulated to four individually calibrated treatment vessels located directly before the four bioreactors (Fig. 1). A pump in each treatment vessel fed the associated downstream bioreactor over a period of less than five minutes on an electronically-controlled schedule either once every hour (Phase I) or twice every hour (Phase II). Inlet and outlet manifolds (5.1 and 10.2 cm diameter PVC, respectively, with drilled holes) spanned the width of each bioreactor at the base of each system. Each outlet manifold connected through the bioreactor downstream wall to a 0.61 m standpipe, which directed outflow into a common sump for the four bioreactors. Flow rates were measured weekly by filling containers of a known volume over a period of one pumping cycle.

2.2. Water quality

Water samples were collected at the influent mixing tank and the four bioreactor outlets. Sample collection timing was initially based on cumulative pore volumes eluted (or, flow volume treated) to normalize between the four HRT treatments. Thus, over the first 47 d (or approximately 20 cumulative pore volumes for the slowest flow rate treatment that was operating under a 55 h HRT), samples were collected relatively frequently but not necessarily at the same time for all four bioreactors. Beyond this day, samples were collected concurrently every week. All samples were analyzed onsite for COD, carbonaceous biochemical oxygen demand ($cBOD_5$), and TSS following standard methods (APHA, 2005; Hach, 2003). Removal efficiencies (%) for COD, $cBOD_5$, TSS, and NO_3^--N were calculated as the influent concentration minus the effluent concentration divided by the influent concentration (see Table 1 for mean influent concentrations). Removal rates for COD and TSS (g COD or TSS removed m^{-3} bioreactor d^{-1}) were calculated as the difference in influent and effluent concentrations times the bioreactor flow rate divided by the total bioreactor volume (length × width × depth of woodchips; 2.21 m^3).

Water samples were also collected from 5 cm diameter PVC monitoring wells located 0.18, 1.74, and 3.57 m from the bioreactor upstream wall in each bioreactor (Fig. 1) on d 120 and 188, which provided information for Phases I and II, respectively. The depth to water was measured in each well (Geotech Environmental Equipment, Keck Water Level Meter) before and after purging a volume of no less than approximately three times the monitoring well volume (or, no less than 3000 mL) using a peristaltic pump (MasterFlex L/S Model 7018-20). Well samples were analyzed for TSS, NO_3^--N, and sulfate (SO_4^{2-}) following standard methods (APHA, 2005; Hach, 2003).

2.3. Flow dynamics

A pressure transducer suspended in the inlet pipe just above the bioreactor floor in each bioreactor logged the depth of water in this pipe every minute (Fig. 1; Solinst Levelogger Model 3001). Data from the four transducers were downloaded weekly and a representative 7 h period was selected for analysis for each bioreactor for each week. Data were corrected for barometric pressure (Solinst Barologger Edge, Model 3001; Solinst Levelogger Software 4.0) and normalized to the outlet standpipe elevation (i.e., 60 cm saturated depth). The pressure transducers were cleaned weekly per manufacturer's instructions to remove bacterial growth. One way analysis of variance (ANOVA) testing was used to evaluate changes in the time required for the pumped volume to move from this inlet pipe into the woodchips across the first 24 wk of operation (Sigma Plot 12.5).
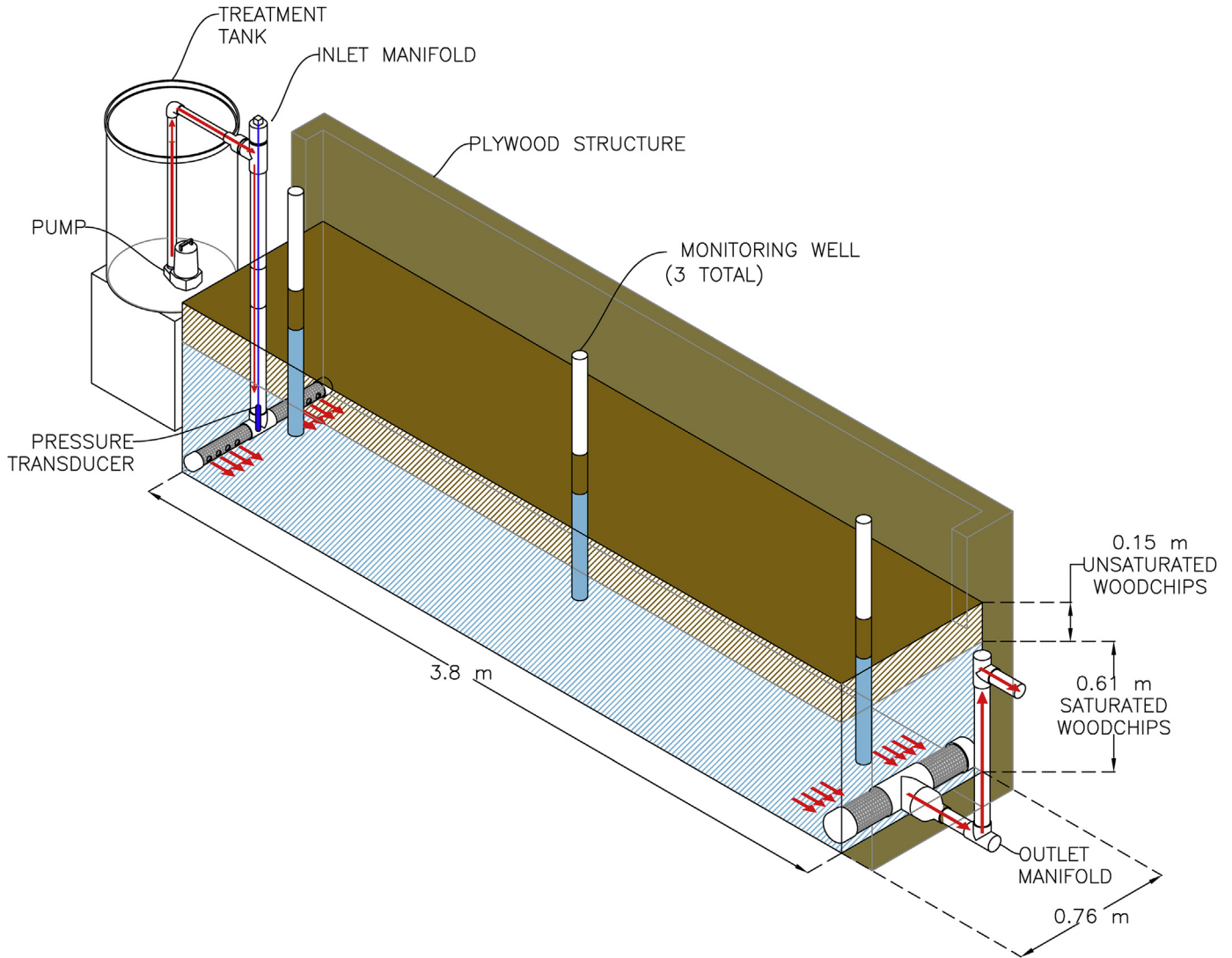
Fig. 1. A cut-away view of one of four pilot-scale woodchip bioreactors with its associated inflow pump, three monitoring wells, and inlet (with suspended pressure transducer) and outlet manifolds. Flow direction indicated with red arrows. (For interpretation of the references to colour in this figure legend, the reader is referred to the web version of this article.)

Tracer tests were conducted in each bioreactor during start-up (prior to d 20), towards the end of Phase I (d 125–149), and at the end of Phase II (days 257–264). These tests gave an indication of the actual residence time of each bioreactor (t, tracer residence time, Eq. (2); Tchobanoglous et al., 2003), and helped identify the potential for short-circuiting, dead zones, and other non-plug flow hydraulics.

Table 1
Influent wastewater water quality parameters (mean ± SD (number of samples)) for the duration of the pilot-scale bioreactor study.

Water quality parameter	Influent mean
Chemical oxygen demand (mg COD/L)	138.5 ± 85.4 (67)
Carbonaceous biochemical oxygen demand (mg cBOD$_5$/L)	37.4 ± 12.7 (37)
Total suspended solids (mg TSS/L)	63.7 ± 44.0 (49)
Nitrate-Nitrogen (mg NO$_3^-$-N/L)[a]	48.3 ± 26.5 (86)
Total Nitrogen (mg N/L)[a]	52.5 ± 23.1 (67)
Sulfate (mg SO$_4^{2-}$/L)[a]	76.8 ± 27.0 (48)

[a] See Lepine et al. (2016) for more discussion.

$$t \approx \frac{\sum t_i C_i \Delta t_i}{\sum C_i \Delta t_i} \qquad (2)$$

Where t_i and C_i were the time and tracer concentration, respectively, of the ith sample, and Δt_i was the time increment between measurements (Tchobanoglous et al., 2003). A slug of no more than 0.25 kg NaCl/L was added to a given bioreactor during one pumping cycle in a pumped volume of either 22, 28, 51, or 100 L for bioreactors 4 through 1, respectively (i.e., treatment vessel volume). Sodium nitrate at a concentration of approximately 30–70 mg NO$_3^-$-N/L was also added to the tracer solution to avoid diluting NO$_3^-$ dynamics during testing. At the given hour, the valve connecting a given bioreactor's treatment vessel to the upstream mixing tank was shut, and the treatment tank was filled with the pre-mixed tracer solution. An initial salinity measurement was taken from the treatment vessel and effluent samples were then assessed for salinity over time to determine the tracer curve (YSI Salinity meter Model 30). Effluent samples were collected by hand for the first tracer test; the subsequent two tracer tests utilized an autosampler

(Teledyne ISCO 6712). The ratio of the tracer residence time to the flow-rate based HRT was the effective volume ($e = t/\tau$) (Thackston et al., 1987). If e is less than one, (that is, if the tracer elutes before expected based on the HRT), short circuiting may be occurring because dead zones reduce the active reactor volume. The tests were designed to capture three to four pore volumes, and total elution took from 46 to 184 h depending on the retention time treatment.

2.4. Woodchip nutrient and fiber content

Forty-eight woodchip media bags were deployed during bioreactor filling to capture the changes in woodchip nutrient (N, C, phosphorus (P)) and fiber (lignin, cellulose, hemicellulose) content over the experiment. Media bags consisted of 30 cm squares of polyester drain sleeve fabric filled with approximately 200 g air-dried woodchips, zip-tied closed, and marked with identifying tag numbers. Twelve bags were placed in each reactor, with six bags within the bottom 5 cm (saturated conditions) and six in the top 5 cm (unsaturated, aerobic conditions). At each depth, two bags were near the inlet manifold, two near the center, and two near the outlet manifold. Six bags from each reactor were removed between d 41 and 63 (i.e., "50 ± 10 d" bags; one from each top/bottom and inlet/middle/outlet placement combination). Cords tied to the bags that extended to the bioreactor surface facilitated bag removal, though some digging was required for the deeper placed bags. The

second set of six bags was harvested at the end of the experiment ($\approx$ d 267; "267 d" bags). The bags were sent to an external lab (Agri-Analysis Labs, Inc., Lancaster, PA) for analysis for phosphorus (% P_2O_5), % N, % C, acid detergent fiber (% ADF), neutral detergent fiber (% NDF; ANKOM Fiber Analyzer), and lignin (% lignin; Klason Lignin Method). Cellulose content was calculated as ADF content minus lignin, and hemicellulose content was calculated as NDF content minus ADF. The lignocellulose index (LCI) was the lignin content divided by the lignin + cellulose content. Changes in nutrient and fiber content over time and between top/bottom-placed woodchips or along longitudinal placement within the bioreactors were assessed with ANOVA testing; normally and non-normally distributed data were evaluated with one way ANOVA testing and Kruskal-Wallis ANOVA testing based on rank, respectively (Shapiro-Wilk normality test; Sigma Plot 12.5).

3. Results and discussion

3.1. Water quality

3.1.1. COD and cBOD5

Woodchip leaching initially negated any COD removal, but all bioreactors eventually transitioned to positive removal at days 40, 47, 85, and 113 for Bioreactors 1 through 4, respectively (Fig. 2a, days noted with arrows). These days equated to cumulative pore volumes of 78, 46, 51, and 47 for the four bioreactors, respectively
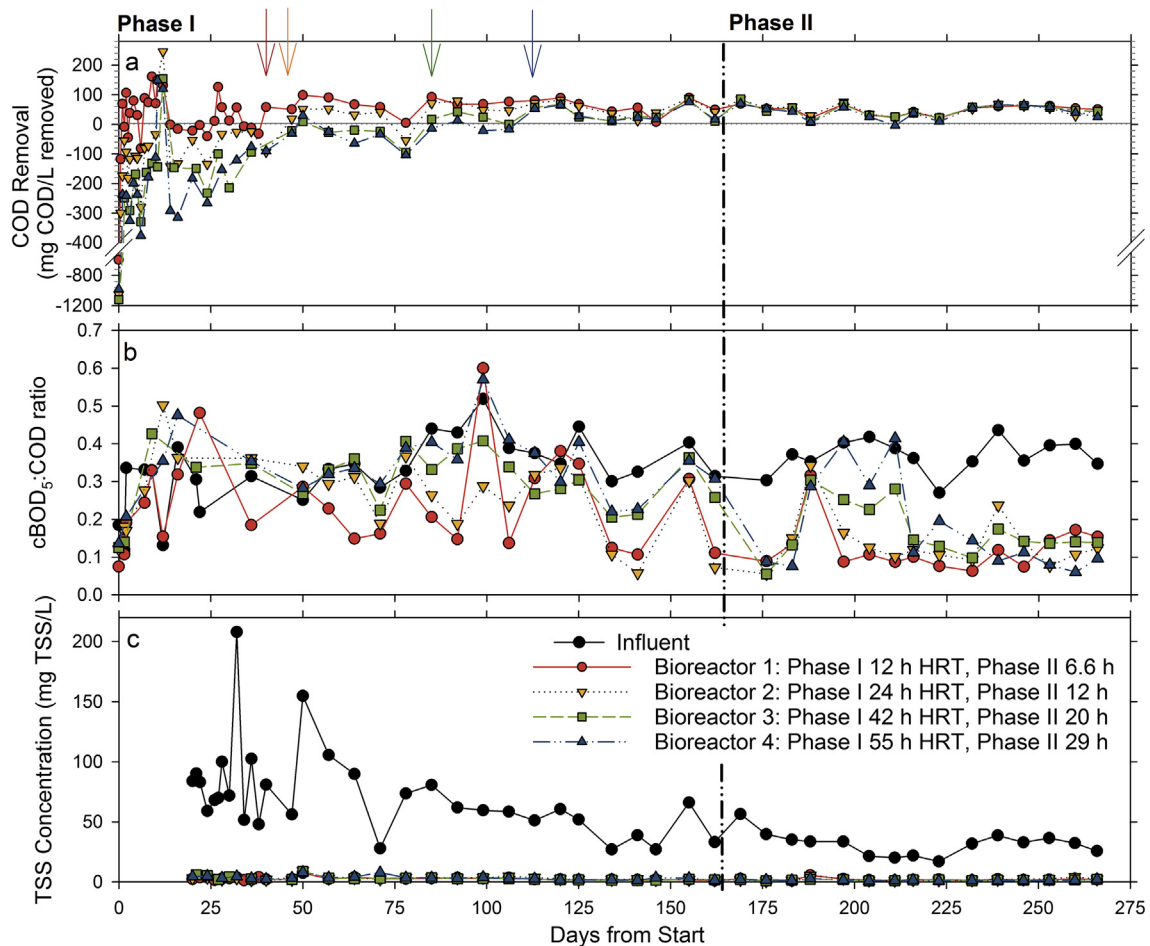

Fig. 2. Chemical oxygen demand removal (a; influent minus effluent concentration), ratio of cBOD5:COD (b), and TSS concentrations (c) from four pilot-scale woodchip bioreactors; arrows in (a) indicate when the effluent COD concentrations began to be consistently lower than the influent for the four retention time treatments.
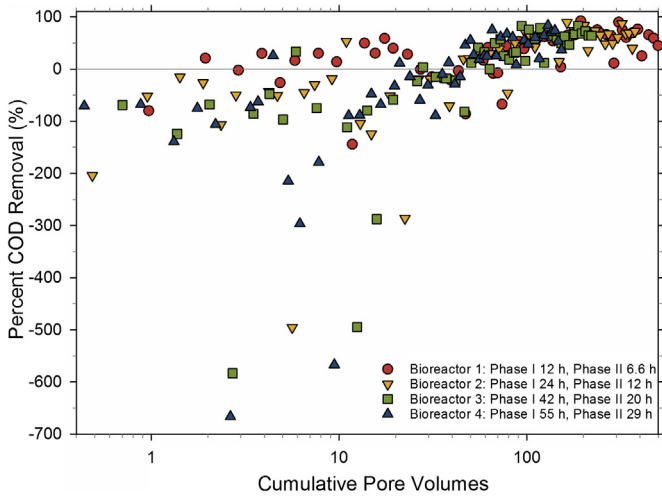
Fig. 3. Chemical oxygen demand (COD) removal efficiency for four aquaculture wastewater treatment bioreactors operated at different hydraulic retention times when normalized by cumulative flow treated (log scale).

(97, 57, 63, and 58 m^3 of wastewater treated, respectively). Thus, COD flushing was over sooner with a faster flow rate, but took fewer cumulative pore volumes with a slower flow rate. Regardless, COD start-up flushing required roughly between 45 and 80 cumulative pore volumes for all treatments. While this was a greater number of pore volumes than extrapolated from work by Healy et al. (2012) (300 d divided by 13–17 d retention time ≈ 20 cumulative pore volumes required for their pine chips), it still appeared to be a reasonably short period considering the life of woodchip bioreactors is typically expected to be at least 5–10 yr (Schipper et al., 2010). It is well established that woodchips leach organics during woodchip bioreactor start-up (Cameron and Schipper, 2010; Fowdar et al., 2015), and suggested leaching

minimization strategies include use of higher carbon: nitrogen (C:N) bioreactor fill media, pre-flushing the media, or starting-up the bioreactor under high flow conditions for dilution of initial outflow. These results confirm flushing of woodchip-sourced COD will dissipate sooner under higher flow rates.

The maximum COD concentrations leached were greater than 400% of the influent (Fig. 3) or greater than 1000 mg COD/L (Fig. 2a). Influent COD generally ranged from 47 to 360 mg COD/L (Table 1). The greatest COD production (i.e., negative removal) originated from slower flow rate treatments due to either internal cycling of waste solids or to sulfate reduction occurring in these long HRT treatments which Robertson et al. (2005) observed was correlated with an increase in bioreactor effluent BOD concentrations.

When the start-up flushing prior to d 113 was excluded from analysis, modeled COD removal was 56% and 25 g of COD removed per m^3 of bioreactor per d at the design HRT of approximately 24 h recommended by Lepine et al. (2016) for treatment of this water chemistry (Fig. 4a and b). Removal efficiency and removal rates of COD were lower at longer HRTs, indicating short design HRTs will maximize COD removal. Saliling et al. (2007) previously documented woodchip bioreactors were capable of COD removal at the lab-scale, but this was the first attempt to quantify both COD leaching and removal under different flow regimes.

Influent cBOD$_5$ generally ranged from 20 to 65 mg cBOD$_5$/L, and effluent concentrations averaged 53.0 ± 39.4 and 7.1 ± 6.9 mg cBOD$_5$/L before and after day 113, respectively (data not shown; recall, d 113 was the final day of COD flushing in Fig. 2a). Removal of cBOD$_5$ averaged 76 ± 23% across all bioreactors following d 113 and 90 ± 3.6% during the final month of testing. The influent wastewater ratio of cBOD$_5$:COD over the duration of bioreactor operation was 0.34 ± 0.08, indicating relatively low biological availability (Fig. 2b). A BOD:COD ratio of greater than 0.5 indicates wastewater is easily treated by biological methods, whereas ratios less than 0.3 require acclimated bacteria for stabilization (Tchobanoglous et al., 2003). Note, ratios here were carbonaceous BOD:COD, thus were
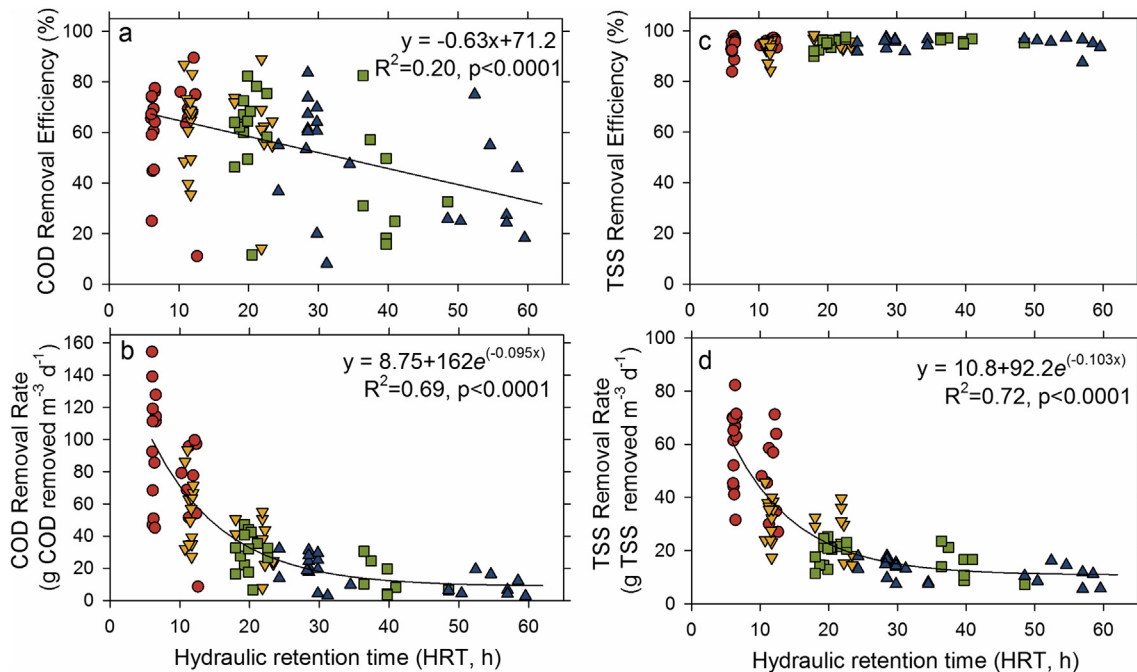

Fig. 4. Hydraulic retention time versus COD and TSS removal efficiency (a, c) and removal rate (b, d) for sampling events beyond day 113 of bioreactor operation to remove start-up flushing effects; figure symbols correspond with the four bioreactors as shown in the legend of Fig. 3.

likely a little lower than would have been expected for a standard BOD:COD ratio that includes nitrogenous BOD. Bioreactor effluent tended to have lower cBOD$_5$:COD ratios than the influent, which may have indicated (1) biodegradable matter in the wastewater was being removed across the bioreactors and/or (2) the leached constituents from the woodchips were not highly biodegradable and thus diluted the biodegradability of the effluent solution. Towards the end of the tests, effluent COD consistently comprised approximately 5–25% cBOD$_5$ (Fig. 2b).

3.1.2. TSS

TSS removal was nearly complete regardless of flow treatment or hydraulic loading (Fig. 2c; Fig. 4c). Beyond day 113 (to avoid start-up flushing effects), TSS removal rates were greatest at short HRTs and highest loadings (Fig. 4d), but removal efficiencies were high across all HRTs, and did not appear to differ between treatments (Fig. 4c). Removal of TSS occurred primarily near the inlet (Fig. 5a; i.e., within 20 cm from the bioreactors' upstream wall), but over a period of roughly ten wk, this settling front appeared to migrate downstream (Fig. 5 a vs b; sampling dates of 120 and 188 d). By 188 d, the highest flow rate treatment resulted in notably altered hydraulics (i.e., ponding near the bioreactor inlet; 507 m^3 water treated; 409 cumulative pore volumes). The elevated TSS concentration observed at the inlet well for this bioreactor (Fig. 5b

Bioreactor 1) was evidence of ponded, high-solids water near the inlet. The slightly elevated TSS concentration near the inlet of Bioreactor 2, which received the second highest loading rates (Fig. 5b Bioreactor 2), may have been early evidence of similar hydraulic problems.

3.1.3. Internal nitrate and sulfate cycling

At both relatively high and low influent NO$_3^-$-N concentrations, N removal was rapid within the bioreactors with concentration reductions of generally greater than 70% by the middle of the bioreactors (Fig. 5 c and d, neglecting Bioreactor 1 in Fig. 5c). This middle point corresponded with roughly half of the design HRT for these bioreactors, or 6, 12, 21, and 28 h HRT for bioreactors 1 through 4, respectively, during Phase I (and 3.3, 6, 10, and 15 h HRT in Phase II). Thus, at an influent of only 17 mg NO$_3^-$-N/L with this wastewater, an HRT of less than 6 h may have been sufficient for complete NO$_3^-$ removal (Fig. 5d; influent loading: 0.7–3.4 g NO$_3^-$-N/h), but at a greater loading more consistent with typical recirculating aquaculture system effluents, more than 24 h was required for 100% removal (Fig. 5c; influent loading: 1.6–7.2 g NO$_3^-$-N/h).

Sulfate reduction was observed to a greater extent in the bioreactors operated under long HRTs that also achieved nearly complete NO$_3^-$ removal (Fig. 5e and f). Though NO$_3^-$ removal was nearly complete in Bioreactor 2 during both well sampling events, sulfate
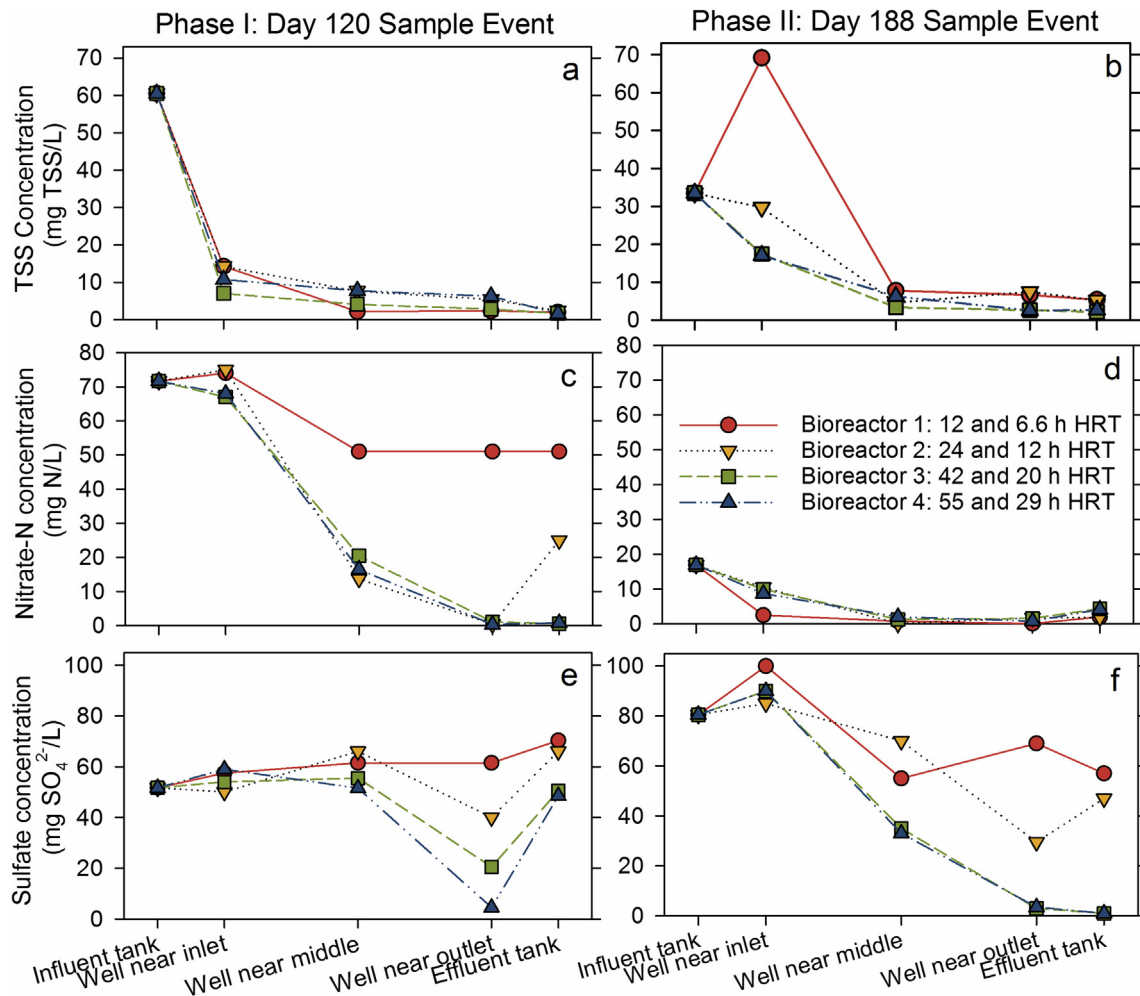

Fig. 5. Concentrations of total suspended solids, nitrate-N, and sulfate from monitoring wells near the bioreactor inlet, middle, and outlet (0.18, 1.74, and 3.57 m from the upstream wall, respectively) for four bioreactors each operated at a different retention time during two testing phases (see legend for hydraulic retention times).
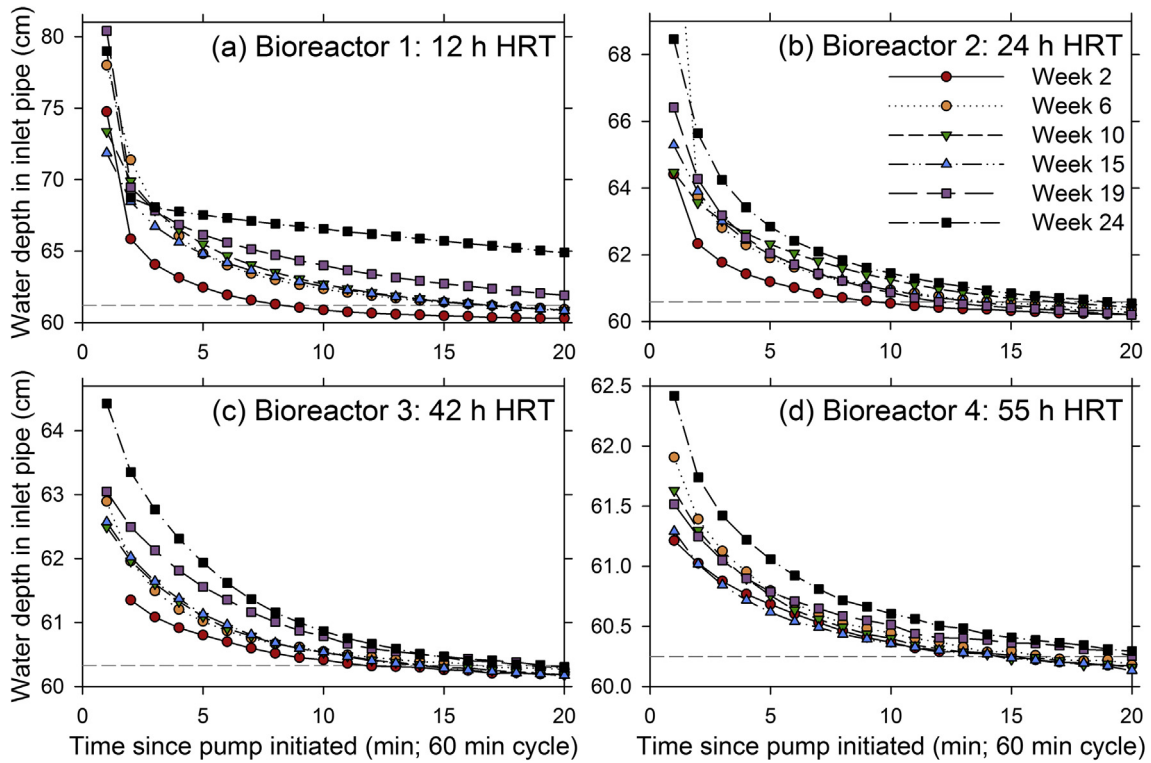
Fig. 6. Water depth in the inlet standpipe following the hourly pumping cycles over the first 24 wk of bioreactor operation; each line reflects the mean of $n = 7$ consecutive hourly pumping cycles per bioreactor per wk; y-axis scales vary by panel due to different HRTs; horizontal dashed line indicates the equivalent depth in the inlet pipe for 0.025% of the pumped volume for each bioreactor.

reduction there occurred to a lesser degree than in Bioreactors 3 and 4 that were operating under longer HRTs. During the first sample event, aeration of the effluent as it exited the bioreactor outlet standpipe may have potentially caused reduced forms of sulfur in the bioreactor solution (i.e., sulfide) to oxidize back to sulfate.

3.2. Flow dynamics

3.2.1. Reactor pumping hydraulics

Water depths recorded every minute in the bioreactors' inlet pipes showed the wastewater took progressively longer to move into the woodchips over the first ≈162 d of operation (Fig. 6). For example, during the second and 19th weeks of operation, Bioreactor 1 had 60.9 and 64.0 cm of water, respectively, remaining the inlet pipe 10 min following the influent pumping (Fig. 6a). The time for the vast majority of the treatment liquid (99.975% of volume) to move into the bioreactor each hour (that is, the remaining 0.025% of 100, 51, 28, and 22 L is 25, 13, 7, and 5 mL, divided over the 5 cm

diameter inlet pipe surface area yields 1.2, 0.6, 0.33, and 0.25 cm equivalent depth remaining in the inlet pipe depth; Table 2) significantly increased over the first 24 wk of bioreactor operation (Table 2). It is likely these changes were due to a combination of (1) woodchip settling, (2) clogging due to removed wastewater solids and/or accumulated bacterial growth, and/or (3) the pulsed flow system pushing the chips away from the inlet, which was particularly observable in Bioreactor 1 as it received the highest loading. Ponding that appeared near the inlet of Bioreactor 1 eventually migrated downstream to affect the entire bioreactor by the end of testing, although NO_3^- removal was still observed (Fig. 5d).

3.2.2. Tracer tests

Generally when the tracer residence time and theoretical HRT (Eqs. (2) and (1), respectively), varied by more than ±10% (or, outside of the gray shading surrounding the 1:1 line in Fig. 7), the tracer residence time was shorter than the flow-rate based HRT (i.e., points fell beneath the 1:1 line). This ratio of tracer residence time to theoretical HRT, or the effective volume (Eq. (3), e) is less

Table 2
Required time (min) to achieve entry of 99.975% of each bioreactors' predefined treatment volume into the bioreactor (i.e., time at which only 0.025% of volume remained in the inlet pipe); Means followed by the same letter within a given row are not significantly different at $\alpha = 0.05$ ($n = 7$ pumping cycles); letters do not apply to comparisons within columns (i.e., statistics were not run comparing across the four bioreactors for a given week).

	0.025% of pumped volume mL	Equivalent depth in pipe cm	Wk 2	Wk 6	Wk 10	Wk 15	Wk 19	Wk 24
			min					
Bioreactor 1: 12 h HRT	25	61.20	9.0 d	17.7 c	17.6 c	17.6 c	27.3 b	45.1 a
Bioreactor 2: 22 h HRT	13	60.60	9.6 e	14.7 c	16.9 b	13.9 cd	12.7 d	19.3 a
Bioreactor 3: 42 h HRT[a]	7	60.33	12.4 b	16.7 ab	14.6 ab	14.4 ab	20.0 a	19.1 a
Bioreactor 4: 55 h HRT[a]	5	60.25	14.4 b	16.6 ab	14.7 b	15.1 ab	21.0 ab	22.6 a

[a] Non-normally distributed data; analyzed using Kruskal Wallis one-way analysis of variance based on rank.
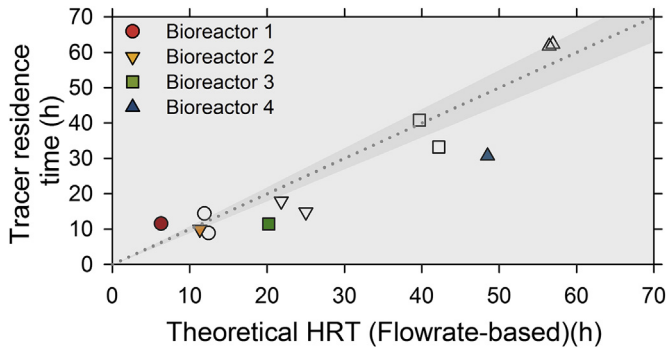
Fig. 7. Theoretical hydraulic retention time versus tracer test residence time of four pilot-scale woodchip bioreactors; the two open symbols for each bioreactor were for the two Phase I tracer tests, while the filled symbol represents the Phase II tracer test; 1:1 relationship ± 10% shown with dotted line and gray shading.

than one if short circuiting is occurring, because dead zones reduce the active reactor volume. Here, e averaged 0.83 ± 0.21 (Mean ± StDev) for bioreactors 2, 3, and 4, signifying roughly 83% of each bioreactor was contributing to the active flow volume. This indication of short circuiting was corroborated by the relatively early tracer peaks that occurred at 0.22 ± 0.10 (mean ± StDev) cumulative pore volumes for these three bioreactors; an ideal tracer curve peaks at one eluted pore volume. Short-circuiting has previously been observed in a non-ideally functioning field-scale woodchip bioreactor ($e < 0.60$, Christianson et al., 2013).

The major exception to this short-circuiting was Bioreactor 1

that experienced the most altered hydraulics over 10 mo of operation (e.g., Fig. 6a). The effective volume for this bioreactor increased over the three tracer tests from 0.72 (t and τ of 8.9 and 12.4 h, respectively) to 1.21 (14.4 and 11.9 h, respectively) to 1.83 (11.5 and 6.3 h, respectively). While the first tracer test indicated relatively similar hydraulics to the other bioreactors (e of 0.72 vs. 0.83), as Bioreactor 1 became increasingly ponded, the flow regime changed. Ghane et al. (2015) and Cameron and Schipper (2012) documented $e > 1.5$ in woodchip bioreactors which indicated a physical or chemical retardation of the tracer. Such tracer retardation was also the case for Bioreactor 1 with this impact seemingly increasing over time. While short-circuiting was noted in Bioreactor 2 (i.e., $e < 1.0$), the e similarly increased over the three tracer tests, though not to the same extent as Bioreactor 1 (e increased from 0.59 to 0.82 to 0.88 over the three tests). This generally corroborated early signs of clogging in Bioreactor 2 compared with Bioreactors 3 and 4 (e.g., Fig. 5b), which had no consistent trend for e.

3.3. Woodchip media

Between d 50 and 267, woodchip C, N, P_2O_5, and cellulose content typically increased, while lignin content relatively decreased at all bag depths and longitudinal locations (Tables 3 and 4). The top placed bags became significantly enriched with relatively greater percentages of C and N over time, and the bottom placed bags underwent a significant increase in C, but not N content (Table 3). The significant increase in N content of the top bags (0.34–0.51%N) likely drove the corresponding significant decrease

Table 3
Woodchip nutrient and fiber composition from top-versus bottom-placed bags at 50 ± 10 d and at the end (267 d) of pilot-scale bioreactor operation; Means followed by the same letter within a given row are not significantly different at $\alpha = 0.05$; $n = 12$ as inlet, middle, and outlet bag values were averaged for each depth for each sample date (3 bags per bioreactor per sample date = 3 × 4 bioreactors = 12). C:N is the carbon to nitrogen ratio; LCI is the Lignocellulose Index.

	Initial ($n = 1$)	Top bags			Bottom bags		
		50 ± 10 d	267 d	% change[c]	50 ± 10 d	267 d	% change[c]
C%[a]	51	52(2.8) bc	55(1.3) a	5.6	52(2.3) c	55(1.6) ab	5.6
N%[a]	0.19	0.34(0.12) b	0.51(0.16) a	51	0.28(0.04) b	0.35(0.06) ab	27
C:N[a]	275	168(41) a	124(60) b	−26	193(30) a	161(28) ab	−16
% P_2O_5[a]	0.031	0.06(0.04) bc	0.13(0.11) ab	127	0.04(0.01) c	0.12(0.10) a	192
Lignin[b]	16.9	17.7(1.2)a	15.7(1.9)b	−12	17.9(1.8)a	14.5(1.9)b	−19
Cellulose[b]	56	55(2.0)b	55(3.3)ab	1.2	56(2.7)ab	58(3.0)a	4.8
LCI[b]	0.20	0.24(0.02)a	0.22(0.02)ab	−9.9	0.24(0.03)a	0.20(0.03)b	−18

[a] Non-normally distributed data; Kruskal-Wallis One Way Analysis of Variance on Ranks.
[b] Normally distributed data; One Way ANOVA.
[c] Percent change between the means of the two sample dates (d = 50 and 267).

Table 4
Woodchip nutrient and fiber composition from in-, middle- or outlet-placed bags at 50 ± 10 d and at the end (267 d) of pilot-scale bioreactor operation; Means followed by the same letter within a given row are not significantly different at $\alpha = 0.05$; $n = 8$ as top- and bottom-placed bag values were averaged for each longitudinal location for each sample date (2 bags per bioreactor per sample date = 2 × 4 bioreactors = 8). C:N is the carbon to nitrogen ratio; LCI is the Lignocellulose Index.

	Initial ($n = 1$)	Near inlet			Middle			Near outlet		
		50 ± 10 d	267 d	% change[c]	50 ± 10 d	267 d	% change[c]	50 ± 10 d	267 d	% change[c]
C%[a]	51	52(3.1) b	55(1.2) ab	5.8	51(2.0) b	56(0.6) a	8.9	54(1.9) ab	55(1.9) ab	2.1
N%[a]	0.19	0.34(0.11) ab	0.45(0.14) a	34	0.31(0.10) ab	0.44(0.17) ab	40	0.27(0.04) b	0.40(0.14) ab	49
C:N[b]	275	165(40) ab	131(37) b	−20	173(35) ab	141(44) ab	−18	205(28) a	156(67) ab	−24
% P_2O_5[a]	0.031	0.07(0.04) ab	0.19(0.13) a	186	0.05(0.03) ab	0.09(0.08) a	88	0.03(0.01) b	0.10(0.06) a	197
Lignin[b]	16.9	17(1.7) ab	15(1.3) b	−15	18(1.3) a	16(2.7) ab	−14	18(1.6) a	15(1.7) b	−17
Cellulose[d]	56	56(3.0)	58(3.8)	2.5	54(1.8)	57(3.5)	4.5	56(1.9)	57(3.4)	2.2
LCI[b]	0.20	0.24(0.02)abc	0.20(0.02)c	−14	0.25(0.02)a	0.22(0.04)abc	−13	0.24(0.02)ab	0.21(0.02)bc	−15

[a] Non-normally distributed data; Kruskal-Wallis One Way Analysis of Variance on Ranks.
[b] Normally distributed data; One Way ANOVA.
[c] Percent change between means of the two sample dates (d = 50 and 267).
[d] There was no statistically significant difference in cellulose content between sample dates (p = 0.319).

in C:N ratio of those bags (168—124 C:N), which was a notable decline from the initial C:N of 275 for these chips (Table 3). This relative N enrichment indicated the top-placed bags, which were in the unsaturated top 15 cm of the bioreactors, were potentially degrading more so than the bottom-placed bags. Moorman et al. (2010) similarly reported aerobic woodchips near the top of a denitrification wall had a shortened life compared to deeper-placed, more consistently anaerobic chips. Along the bioreactors' longitudinal axes, C:N ratio decreases over time were not significant at any of the three locations (Table 4).

Woodchip P_2O_5 content increased over time generally by at least two-fold regardless of depth or longitudinal placement (Tables 3 and 4), and this increase was significant in the outlet-placed and bottom-placed bags (0.03 vs 0.10%P_2O_5, Table 4; 0.04 vs. 0.12%P_2O_5, Table 3). Increasing P content of the woodchip media corroborated previous conclusions by Sharrer et al. (2016) that filtration of wastewater solids was a major contributor to observed total phosphorus removal from the wastewater.

The lignin content decreased significantly over time for both top- and bottom-placed bags (Table 3) and in the bags placed near the outlet (Table 4). Schmidt and Clark (2013) similarly showed a decrease in lignin content for hardwood media over 246 d in denitrification column studies, although lignin content increased over time for their softwood (pine) treatments. Driven by the lignin changes here, the LCI generally decreased across all bags regardless of location (significant for bottom placed bags, 0.24 to 0.20; Table 4), which was contrary to expected increases in LCI as cellulose is utilized and the media becomes increasingly recalcitrant (i.e., lignin should become a greater proportion of the media over time). Both Feyereisen et al. (2016) and Schmidt and Clark (2013) reported LCI increased over time in woodchips (0.45 increased to 0.47 and 0.25 increased to 0.44, respectively). The unexpected decrease here may have been due to settled C-based solids that became entrapped in the woodchips. If so, this helps corroborate the difference in $cBOD_5$:COD ratio between the influent and effluent (i.e., biodegradable cellulosic matter in the wastewater was being removed across the bioreactors, Fig. 2b).

4. Conclusions

Wastewater treatment in a denitrification woodchip bioreactor presents potential for reduced hydraulic capacity and woodchip clogging compared to other applications of this technology typically associated with lower TSS and COD inlet concentrations (e.g., drainage water, groundwater). This problem is two-fold: (1) solids filling the system may result in eventual plugging, thus shortening the life of the reactor, and (2) as the solids are entrapped, they degrade and mineralize releasing biologically available nutrients of concern like phosphorus (although mineralization may also provide readily biodegradable organic acids to drive denitrification). One of the strongest pieces of evidence for this was that TSS removal efficiencies were generally >90% due to filtration by the woodchips which occurred primarily near the inlet. Additionally, wastewater took significantly longer to move into the bioreactors over time particularly under the highest loading conditions. While a gravity thickening settler was upstream of these pilot-scale bioreactors, an additional microscreen filter could be used for pretreatment in this application. Such a "treatment-train" approach will help extend the life of the bioreactor and reduce complications of nutrient mineralization.

There were notable HRT impacts upon start-up COD flushing, eventual COD and TSS removal, and potential clogging. Chemical oxygen demand flushing was over sooner with a faster flow rate, but required fewer cumulative pore volumes (roughly 50 vs. 80) under a slower flow rate. Designing for relatively shorter HRTs

optimized COD and TSS removal rates, and such designs will also optimize COD removal efficiency. Nitrate removal persisted across the duration of the tests predominantly on the bioreactors' inlet side, even for the bioreactor with the most altered hydraulics. The excellent N and TSS removal along with notable COD removal indicated woodchip bioreactors are a viable water treatment technology for these types of wastewaters given that they are used downstream of a filtration device (e.g., recommended additional microscreen filter mentioned above) and under HRTs of at least 24 h. Woodchip bioreactor lifespan is unknown in this application, but it is likely that relatively more frequent media replacement than is typically recommended (i.e., sooner than 5—10 yr) may be required for high COD and TSS applications.

References

APHA, 2005. Standard Methods for the Examination of Water and Wastewater, twenty-first ed. American Public Health Association, Washington, DC.

Cameron, S.G., Schipper, L.A., 2010. Nitrate removal and hydraulic performance of organic carbon for use in denitrification beds. Ecol. Eng. 36, 1588—1595.

Cameron, S.G., Schipper, L.A., 2012. Hydraulic properties, hydraulic efficiency and nitrate removal of organic carbon media for use in denitrification beds. Ecol. Eng. 41, 1—7.

Christianson, L., Helmers, M., Bhandari, A., Kult, K., Sutphin, T., Wolf, R., 2012. Performance evaluation of four field-scale agricultural drainage denitrification bioreactors in Iowa. Trans. ASABE 55, 2163—2174.

Christianson, L., Helmers, M., Bhandari, A., Moorman, T., 2013. Internal hydraulics of an agricultural drainage denitrification bioreactor. Ecol. Eng. 52, 298—307.

Choudhury, T., Robertson, W.D., Finnigan, D.S., 2016. Suspended sediment and phosphorus removal in a woodchip filter treating agricultural washwater. J. Environ. Qual. 45, 796—802.

Feyereisen, G., Moorman, T.B., Christianson, L.E., Venterea, R.T., Coulter, J.A., Tschirner, U.W., 2016. Nitrate removal, microbial abundance and gas production of agricultural residue media in laboratory denitrifying bioreactors at low temperatures. J. Environ. Qual. 45, 779—787.

Fowdar, H.S., Hatt, B.E., Breen, P., Cook, P.L., Deletic, A., 2015. Evaluation of sustainable electron donors for nitrate removal in different water media. Water Res. 85, 487—496.

Ghane, E., Fausey, N.R., Brown, L.C., 2015. Modeling nitrate removal in a denitrification bed. Water Res. 71, 294—305.

Hach, 2003. DR/4000 Spectrophotometer Procedures Manual, eleventh ed. Hach Company, USA.

Healy, M.G., Ibrahim, T.G., Lanigan, G.J., Serrenho, A.J., Fenton, O., 2012. Nitrate removal rate, efficiency and pollution swapping potential of different organic carbon media in laboratory denitrification bioreactors. Ecol. Eng. 40, 198—209.

Lepine, C., Christianson, L.E., Sharrer, K., Summerfelt, S.T., 2016. Optimizing hydraulic retention times in denitrifying woodchip bioreactors treating recirculating aquaculture system wastewater. J. Environ. Qual. 45, 813—821.

Lu, H., Chandran, K., Stensel, D., 2014. Microbial ecology of denitrification in biological wastewater treatment. Water Res. 64, 237—254.

Moorman, T.B., Parkin, T.B., Kaspar, T.C., Jaynes, D.B., 2010. Denitrification activity, wood loss, and N2O emissions over 9 years from a wood chip bioreactor. Ecol. Eng. 36, 1567—1574.

Robertson, W.D., Ford, G.I., Lombardo, P.S., 2005. Wood-based filter for nitrate removal in septic systems. Trans. ASAE 48, 121—128.

Saliling, W.J.B., Westerman, P.W., Losordo, T.M., 2007. Wood chips and wheat straw as alternative biofilter media for denitrification reactors treating aquaculture and other wastewaters with high nitrate concentrations. Aquac. Eng. 37, 222—233.

Schipper, L.A., Robertson, W.D., Gold, A.J., Jaynes, D.B., Cameron, S.C., 2010. Denitrifying bioreactors—an approach for reducing nitrate loads to receiving waters. Ecol. Eng. 36, 1532—1543.

Schmidt, C.A., Clark, M.W., 2013. Deciphering and modeling the physicochemical drivers of denitrification rates in bioreactors. Ecol. Eng. 60, 276—288.

Sharrer, K., Christianson, L.E., Lepine, C., Summerfelt, S.T., 2016. Modeling and mitigation of denitrification 'woodchip' bioreactor phosphorus releases during treatment of aquaculture wastewater. Ecol. Eng. 93, 135—143.

Tchobanoglous, G., Burton, F.L., Stensel, H.D., 2003. Wastewater Engineering: Treatment and Reuse, fourth ed. McGraw-Hill, London, UK.

Thackston, E.L., Shields, F.D., Schroeder, P.R., 1987. Residence time distributions of shallow basins. J. Environ. Eng. 113, 1319—1332.

von Ahnen, M., Pedersen, P.B., Hoffmann, C.C., Dalsgaard, J., 2016. Optimizing nitrate removal in woodchip beds treating aquaculture effluents. Aquaculture 458, 47—54.

Warneke, S., Schipper, L.A., Matiasek, M.G., Scow, K.M., Cameron, S., Bruesewitz, D.A., McDonald, I.R., 2011. Nitrate removal, communities of denitrifiers and adverse effects in different carbon substrates for use in denitrification beds. Water Res. 45, 5463—5475.

Woli, K.P., David, M.B., Cooke, R.A., McIsaac, G.F., Mitchell, C.A., 2010. Nitrogen balance in and export from agricultural fields associated with controlled drainage systems and denitrifying bioreactors. Ecol. Eng. 36, 1558—1566.